Extended Abstracts of the 2018 International Conference on Solid State Devices and Materials, Tokyo, 2018, pp509-510

SiN Integrated Photonics Platform for Near-Infrared Range Applications

Nicola A. Tyler, Daivid Fowler, Stephane Malhouitre, Stephane Brision, Olivier Lemonnier, Wilfried Rabaud and Bertrand Szelag
University Grenoble Alpes and CEA, LETI, Minatec Campus
F-38054 Grenoble Cedex, France
Phone: +34-4-387-80250 E-mail: nicola.tyler@cea.fr

Abstract

In this article we present a SiN photonic platform for applications in the near-infrared wavelength range of 800-1000 nm. The platform, demonstrated at 940 nm, is composed of low-loss waveguides, splitters, grating couplers and phase-shifters. Furthermore, we demonstrate the possibility of implementing multi-level architectures with low-loss inter-layer coupling.

1. Introduction

Silicon-on-insulator (SOI) photonics has proved to be a successful platform for applications in the telecommunication wavelength bands [1]. Its advantages include CMOS compatibility and a high index contrast, which allows for a high component density. However, as the wavelength transparency of Si is restricted, its applications are limited. SiN on the other hand, has a much broader wavelength transparency (between 500 nm and 3.7 µm [3]) and a refractive index of ~ 2. Its incorporation and use in SOI photonics has emerged in recent years [2], expanding the application scope of SOI-based photonics. Unlike Si, SiN is generally not crystalline, and can be deposited under various conditions, enabling excellent control over the structural properties of the material. Furthermore, SiN is suitable for high-power applications, due to the lack of two photon absorption over a wide wavelength range. The thermo-optic coefficient is approximately one order of magnitude smaller than that of Si [4, 5], resulting in decreased temperature sensitivity.

2. Design and Fabrication Process

A platform based on SiN waveguides embedded in SiO_2 was developed on LETI's 200 mm fabrication platform for applications using light at 940 nm wavelength. In the following, simulations on the waveguide design are presented, succeeded by a description of the fabrication process.

Design criteria

The following design criteria were used: The waveguide dimensions were chosen to be as large as possible in order to minimise the losses due to surface roughness and waveguide bending, while still operating in the monomode regime, guiding the fundamental mode with TE polarisation. In addition, the vertical mode confinement was optimised to allow the lossless addition of metal based heating elements as close as possible to the waveguide.

Waveguide design

A mode solver based on the Finite Element Method (RSoft FemSIM) was used to simulate the effective indices of various modes inside the waveguides. The refractive index values of SiN and SiO_2 were set to 1.99 and 1.456, respectively, based on our ellipsometry measurements. A one-dimensional simulation of the effective indices of the modes inside a SiN slab waveguide was used to approximate the maximum waveguide height for monomode operation, see Fig 1a). It can be seen, that for waveguide heights of ≤ 300 nm, the waveguide supports the fundamental mode (TE_0) only. A waveguide height of 300 nm was chosen and used in the following 2-dimensional simulation to define the optimum waveguide width. Fig 1b) shows that the waveguide is monomode at widths ≤ 600 nm. In order to minimise waveguide losses due to surface roughness, the maximum possible waveguide dimensions in the monomode regime were chosen: 300×600 nm^2. The effective index of the TE mode of a 300×600 nm^2 waveguide was simulated to be 1.68, the electric field intensity distribution is shown in Fig 1c). Constant radius waveguide bending simulations showed losses well below the expected propagation losses for bend radii of ≥ 10 µm (see Fig 1d).

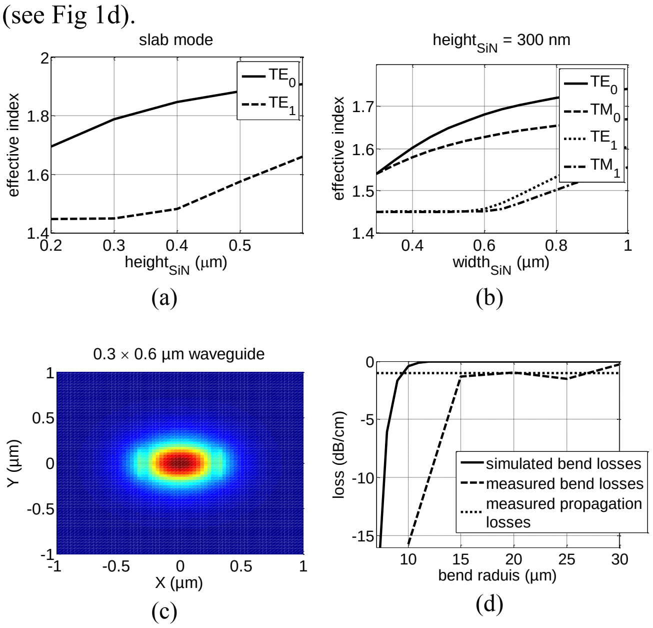

Fig. 1 (a) Simulated effective indices versus SiN slab height for the fundamental and the first order slab mode. (b) 2-dimensional simulation of the effective indices vs. waveguide width for a waveguide height of 300 nm. (c) Intensity distribution of the fundamental mode inside a 300×600 nm^2 waveguide (d) Simulated and measured loss inside curved waveguides.

SiN type and deposition temperature

Both non-stoichiometric Plasma Enhanced Chemical Vapour Deposition (PECVD) SiN_x deposited at 300°C and stoichiometric Low Pressure Chemical Vapour Deposition (LPCVD) Si_3N_4 deposited at 780°C, were evaluated.

Waveguide fabrication

A 1 µm buffer silicon oxide layer was deposited on a 200 nm silicon wafer. Silicon nitride waveguides were patterned in one level using deep ultra violet lithography and plasma dry etching. Finally, a SiO_2 cladding layer was applied.

Phase shifters

A phase shift in SiN waveguides can be achieved using the thermo-optic effect. In order to apply heat to a waveguide element, electrically resistive wires, composed of 1 µm-wide 10/100 nm Ti/TiN here referred to as heaters, were placed at a certain distance above a straight section of waveguide. The distance was chosen so as to be optically lossless, while located close enough to ensure maximum heat transfer. Simulations and measurement indicated an optimum heater-waveguide distance of approximately 800 nm.

4. Test Results

In order to test the performance of the components, measurements on test devices were performed on ~ 40 dies across a 200 mm wafer. The results are presented in the following.

Waveguide losses

The losses of straight waveguides were measured across a wafer using cutback measurements. The best results were obtained for LPCVD Si_3N_4 devices. A median of value of -1.0 dB/cm was found, the measured data across the wafer is shown in Fig 2a). For the PECVD SiN_x waveguides, a slightly higher loss of -1.5 dB/cm was observed. In the following, we will focus on the results of the LPCVD Si_3N_4 platform.

Bend losses

The comparison of measured and simulated bend losses is given in Fig 1d). A bend radius of ≥ 15 µm resulted in a measured loss value similar to that of a straight waveguide, consistent with simulations.

Grating coupler losses

The median fibre-grating coupler loss was determined to be -4.9 dB per coupler, see Fig 2b).

Phase shifters

The functionality of the phase shifters was tested by recording the transmission of a Mach-Zehnder-Interferometer containing a heater in one arm, as a function of heater current. The power corresponding to a π phase shift was found to be independent of the heater length. In the case of the 500 µm long heater, a median of 87 mW of electrical power was found to be necessary to achieve a phase shift of π, see figure 2c).

Interlayer transition

In some applications it may be desirable to work with several vertically stacked layers containing SiN waveguides. We have demonstrated coupling between waveguides of two different layers using inter-layer couplers. An example of such a coupler is illustrated in figure 2d). Two types of couplers were investigated: a short (< 20 µm-long) narrow-band coupler based on evanescent coupling, and a long (~500 µm) wide-band, adiabatic coupler. Various SiO_2 thicknesses between 100 nm and 500 nm separating the SiN layers have

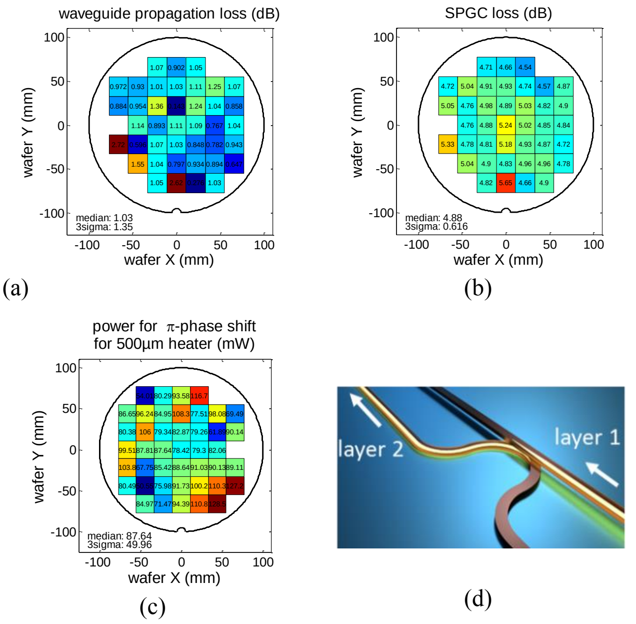

Fig. 2 Measurements on LPCVD Si_3N_4 test structures across a wafer: (a) waveguide loss, (b) grating coupler loss and (d) required heater power for a π phase shift. (d) Illustration of a multi-layer SiN architecture with interlayer coupling.

been tested. Both types of couplers showed losses < 0.1 dB, which is less than or equal to the value of the equivalent length of waveguide due to normal propagation losses.

4. Conclusions

We have demonstrated a low-loss integrated photonic platform based on SiN waveguides for applications at 940 nm, which can be easily adapted for any wavelength in the near-infrared. The process is capable of fabricating multi-layer architectures, and low-loss interlayer coupling was demonstrated. SiN circuits made using this platform are useful for high-power applications outside of the telecommunication bands. We will show our latest results on free space imaging applications using this platform.

References

[1] B. Jalali and S. Fathpour, J. Light. Technol, **24** [12], 4600 (2006).

[2] A. Z. Subramanian, P. Neutens, A. Dhakal, R. Jansen, T. Claes, X. Rottenberg, F. Peyskens, S. Selvaraja, P. Helin, B. Du Bois, K. Leyssens, S. Severi, P. Deshpande, R. Baets, and P. Van Dorpe, IEEE Photonics J, **5** [6], 2202809 (2013).

[3] R. G. F. Baets, A. Z. Subramanian, S. Clemmen, B. Kuyken, P. Bienstman, N. Le Thomas, G. Roelkens, D. Van Thourhout, P. Helin, and S. Severi, Optical Fiber Communication Conference 2016, paper Th3J.1.

[4] A. Arbabi and L. L. Goddard, Opt. Lett. **38** [19], 3878-3881 (2013).

[5] J. Komma, C. Schwarz, G. Hofmann, D. Heinert, and R. Nawrodt, Appl. Phys. Lett. 101, 041905 (2012).